



Title	Theoretical testing of an empirical mode decomposition damage-detection approach using a spatial vehicle-bridge interaction model
Authors(s)	González, Arturo, Meredith, Jill
Publication date	2012-07
Publication information	González, Arturo, and Jill Meredith. "Theoretical Testing of an Empirical Mode Decomposition Damage-Detection Approach Using a Spatial Vehicle-Bridge Interaction Model." Taylor and Francis, July 2012. https://doi.org/10.1201/b12352-56 .
Conference details	6th International Conference on Bridge Maintenance, Safety and Management (IABMAS 2012), Stresa, Lake Maggiore, Italy, 8-12 July, 2012
Publisher	Taylor and Francis
Item record/more information	http://hdl.handle.net/10197/6326
Publisher's version (DOI)	10.1201/b12352-56

Downloaded 2026-05-02 00:25:15

The UCD community has made this article openly available. Please share how this access benefits you. Your story matters! (@ucd_oa)



© Some rights reserved. For more information

Theoretical testing of an empirical mode decomposition damage detection approach using a spatial vehicle-bridge interaction model

J. Meredith & A. González

University College Dublin, Dublin, Ireland

ABSTRACT: Empirical mode decomposition (EMD) is used to detect and locate damage in a bridge using its acceleration response to the crossing of a vehicle. EMD is a technique that converts the measured signal into a number of basic functions that make up the original signal. These functions are obtained purely from the original signal in a sequential procedure, where lower order basic functions contain a range of high frequency components of the signal and higher order basic functions contain the low frequency components. Damage is identified through a distinctive peak in the decomposed signal resulting from applying EMD. Recent studies have shown the potential of this tool to detect single and multiple damages when using the response of a one-dimensional beam model to the crossing of a constant load. In this paper, the technique is further developed using simulations from a quarter-car vehicle-bridge dynamic interaction finite element model. The vehicle model is composed of mass elements, which represent the tyre and body masses, and stiffness and damping elements, which represent tyre and suspension systems. The bridge deck is modelled using plate elements with typical properties found on site and the road profile is generated stochastically from power spectral density functions based on ISO standard guidelines. Different levels of damage are simulated as localised losses of stiffness at random locations within the bridge and a number of longitudinal and transverse locations are used as observation points. The ability of the EMD algorithm to detect damage is analysed for a variety of scenarios including two vehicle configurations (light and heavy), a range of speeds between 5 and 15 m/s, and smooth and rough road surfaces. The influence of the distance from the simulated acceleration points to the damage locations, on the accuracy of the predicted damage, is also discussed.

1 INTRODUCTION

1.1 *Damage detection*

Structural damage detection is a complex and challenging issue in bridge engineering. Its main purpose is to identify the presence, location, type and quantity of damage and predict the remaining service life of the structure. The need for an effective and robust detection method that can be applied to complex structures has led to the development of global damage-identification methods which examine changes in the measured vibration characteristics of the structure. The basic idea behind these methods is that damage will alter the stiffness, mass, or damping properties of a system, and that this change, in turn, will alter the measured dynamic response of the structure (Salvino et al. 2005). Time series analysis is receiving increased attention in the field as it permits vibration signals, from structures, to be decomposed into fundamental basis functions that are used to characterise the vibration response. Wavelet analysis and Empirical Mode Decomposition (EMD), as part of the Hilbert-Huang Transform

(HHT), are two widely researched time-series analysis methods. In contrast to the Fourier transform, which maps from the time domain to the frequency domain, wavelet analysis and EMD may be applied and mapped to the space or time domain of the structure therefore making them capable of damage location.

1.2 *Wavelet analysis*

Wavelet analysis, in recent years, has been one of the emerging and fast-evolving mathematical and signal processing tools for vibration-based analysis. It has been used to locate discontinuities in dynamic measurements that could be associated to structural damage. Kim & Melhem (2004) describe wavelet analysis as the breaking up of a signal into shifted and scaled versions of a mother wavelet or basis function. This results in variable sizes of a window function and makes it possible to detect discontinuities and breakdown points of data. Zhu & Law (2006) first suggested that by performing a continuous wavelet transform (CWT) on the deflection-time

signal of a cracked beam subject to a constant moving load, it was possible to determine the position of the crack. This study however focused on large cracks leading Gonzalez & Hester (2009) to investigate if the method is feasible to identify small cracks and examine the application of a number of wavelet functions for comparison purposes. They concluded that wavelets can be employed to identify damaged sections by using the response of a structure to a moving load. Ayenu-Prah & Attoh-Okine (2009) however highlight that there are complications that arise out of defining *a priori* basis functions, these being that a wavelet based interpretation of a signal is only meaningful relative to the selected mother wavelet. Other disadvantages they mention include spectral leakage and its being non-adaptive. The disadvantages of wavelet analysis prompted the development of a new spectral analysis method called the Hilbert-Huang Transform (HHT).

1.3 Hilbert-Huang transform

The HHT consists of two parts: Empirical Mode Decomposition (EMD) and Hilbert Spectral Analysis (HSA), a full description of which can be found in Huang & Shen (2005). The most notable research and testing into HHT is outlined by Huang (2001) who patented the method. Huang applies HHT to a model of a simply supported bridge with a transient load, designed as a three axle truck. A crack is simulated as a reduction in cross section near the mid-span. The research concluded that, HHT can detect and locate damage, it can estimate the degree of damage and it can be applied to other structures. However the clearest results lay where the undamaged data was used as a comparison.

The use of EMD, on its own, has been recently applied to damage identification in structures subject to dynamic loading. Xu & Chen (2004) conducted experiments, on the use of EMD, using a three storey steel frame building model which was welded to a base plate and bolted to a shaking table. A sudden change of structural stiffness was simulated and signals were acquired using accelerometers. The measured structural response time history was processed, to obtain the first Intrinsic Mode Function (IMF) component, using the EMD approach with intermittency check. This component was then used to identify the damage time instant and damage location of the building. Xu & Chen concluded that the EMD approach can accurately identify the damage time instant by observing the occurrence time of the damage spike in the first IMF component of the acceleration response. They found it to be a useful tool for damage detection in real structures in the sense that it is a signal based and model free method, requiring no prior knowledge on the structure.

Yang et al (2004) performed a similar study employing a four-storey ASCE benchmark building.

They also found that they could detect exact damage locations. They noted that the magnitude of the spikes identifying the damage depends on the external loads, the damage location and the severity of damage.

Recently, Bradley et al (2010) used EMD to detect damage in the acceleration response of a beam model subject to the crossing of a load. This investigation concluded that EMD could be used to detect damage from the accelerations of a structure subject to a moving load. They applied a high-pass filter to the IMFs, resulting from the acceleration response, to detect a single damaged location. It was found that high levels of noise and long beam lengths introduced some small inaccuracies; however, these could be reduced with an increase in observation points. Meredith et al (2011) advanced this research by using a Moving Average Filter followed by EMD to detect multiple damage locations in the acceleration response of a beam model subject to the crossing of a load. This investigation concluded that EMD could be used to detect multiple damage locations from the accelerations of a structure subject to a moving load.

A further study by Meredith & Gonzalez (2011) used simulations based on large samples of moving loads generated stochastically. Velocity and magnitude of the moving loads were generated by applying random sampling to statistics from real Weigh-In-Motion data. The analysis concluded that the response of a structure to everyday traffic (as opposed to the use of a calibrated load of known characteristics) can be used as a tool to identify damage using EMD. It was found that the method could detect small levels of damage with an increase in sensitivity as the number of load crossings is increased.

In this paper, the technique is further developed using simulations from a vehicle-bridge dynamic interaction finite element model. Different levels of damage are simulated as localised losses of stiffness at random locations within the bridge and a number of longitudinal and transverse locations are used as observation points. The ability of the EMD algorithm to detect damage is analysed for a variety of scenarios including two vehicle configurations (light and heavy), a range of speeds between 5 and 15 m/s, and smooth and rough road surfaces. The influence of the distance from the simulated acceleration points to the damage locations, on the accuracy of the predicted damage, is also discussed.

2 VEHICLE-BRIDGE INTERACTION MODEL

For this study, a vehicle-bridge interaction model (VBI) was developed in Matlab 7.11.0 (R2010b). The VBI uses individual models of a bridge, road profile and vehicle that interact with one another to obtain the response of the bridge at a certain point

on it. The response of a discretized FE bridge model to a series of time-varying forces can be expressed by:

$$[M_b]\{\ddot{w}_b\} + [C_b]\{\dot{w}_b\} + [K_b]\{w_b\} = \{f_b\} \quad (1)$$

where $[M_b]$, $[C_b]$ and $[K_b]$ are global mass, damping and stiffness matrices of the model respectively and $\{w_b\}$, $\{\dot{w}_b\}$ and $\{\ddot{w}_b\}$ are the global vectors of nodal bridge displacements and rotations, their velocities and accelerations respectively, and $\{f_b\}$ is the global vector of interaction forces between the vehicle and the bridge acting on each bridge node at time t . Rayleigh damping is used to model viscous damping and is given by:

$$[C_b] = \alpha[M_b] + \beta[K_b] \quad (2)$$

where α and β are constants of proportionality which can be obtained using the relationships:

$$\alpha = \frac{2\zeta\omega_1\omega_2}{(\omega_1+\omega_2)} \quad (3) \quad \beta = \frac{2\zeta}{(\omega_1+\omega_2)} \quad (4)$$

where ω_1 and ω_2 are the first two natural frequencies of the bridge and ζ is the viscous damping ratio (Gonzalez 2011). The damping mechanisms of a bridge may involve other phenomena such as friction, but in this case they are ignored because the levels of damping of a bridge are small and more complex damping modelling would not change the outcome significantly.

2.1 Bridge

For this study the FE model used for modelling the bridge deck is a 2-D plate model (Fig. 1). The bridge is a simply supported, 15 m long and 12 m wide, single span, orthotropic slab.

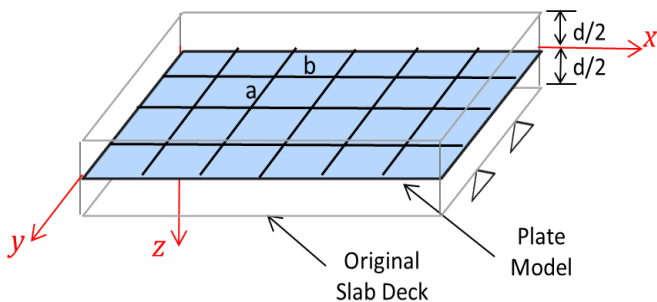


Figure 1. 2-D Plate Model

The bridge model properties, provided in Table 1, are thought to be typical of a bridge of this type (O'Brien et al. 2010). Damage in the bridge is modelled as a percentage reduction in the modulus of elasticity in the longitudinal direction, E_x .

Table 1. Bridge model properties

Longitudinal Modulus of Elasticity (E_x)	3.5×10^{10} N/m ²
Transverse Modulus of Elasticity (E_y)	3.22×10^{10} N/m ²
Shear Modulus (G)	1.4×10^{10} N/m ²
Poisson's Ratio (ν_x, ν_y)	0.2
Damping Ratio (ζ)	0.02
Natural frequencies (ω_1, ω_2)	1.048, 2.084 rads/s
Slab Depth (d)	0.85 m
Element length (a) and width (b)	0.25 m, 0.25 m

2.2 Road Profile

The road profile is generated stochastically from power spectral density functions following guidelines by ISO standards (ISO 8608, 1995). The spectral densities, $G_d(n)$ are given by

$$G_d(n) = G_d(n_0) \left(\frac{n}{n_0}\right)^{-w} \quad (5)$$

where n is the wavenumber in cycles/m, $n_0 = 0.1$ cycles/m and $G_d(n_0)$ and w are constants related to the surface roughness of the pavement. The spectral density is inverse Fourier transformed to produce a discrete set of points representing the profile height, $r(t)$, at regular finite intervals (Harris et al. 2007). Three different road profiles are examined; a perfectly smooth profile, a class 'A' profile ($G_d(n_0) \leq 2 \times 10^{-6}$ m³/cycle) and a class 'B' profile ($2 \times 10^{-6} < G_d(n_0) \leq 8 \times 10^{-6}$ m³/cycle).

Only the paths where wheels will cross are then considered and a profile smoother is applied using a moving average filter of wavelength 24 cm that simulates the tire footprint. An example of a typical class 'A' profile is shown in Figure 2. Vehicles are required to travel a minimum of 100 m on the generated road profile before arriving on the bridge to allow them to reach dynamic equilibrium.

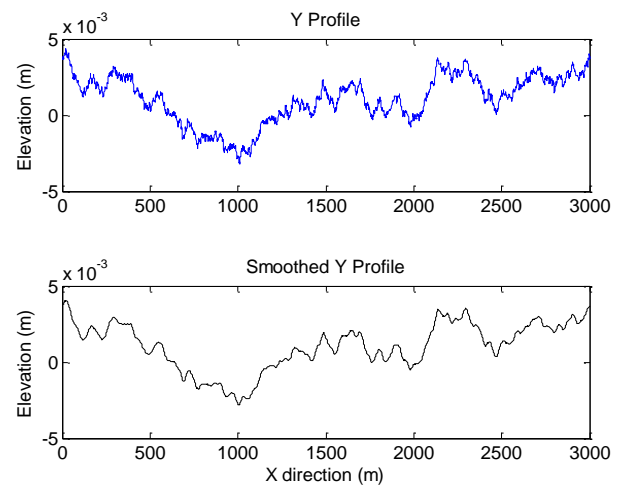


Figure 2. Typical class 'A' road profile

In this investigation, the vehicle model used for simulation of dynamic tyre forces imparted to the

bridge is a quarter-car model (Fig. 3). This is a simple two-DOF model that models two main modes of vibration of the moving load. The suspension consists of a spring with a stiffness coefficient (k_s) of 7.5×10^5 N/m and a damper with damping coefficient (C_s) of 1×10^4 Ns/m. The tyre model has a mass (m_2) of 375 kg with a stiffness coefficient (k_w) of 1.2×10^6 N/m. The sprung mass of the quarter-car (m_1) is varied from light to heavy loads. The car is deemed to be moving, from left to right, along a path 3 m from the edge of the bridge, which is the equivalent to the centre line of one lane (the 12 m wide bridge is assumed to carry two lanes of traffic).

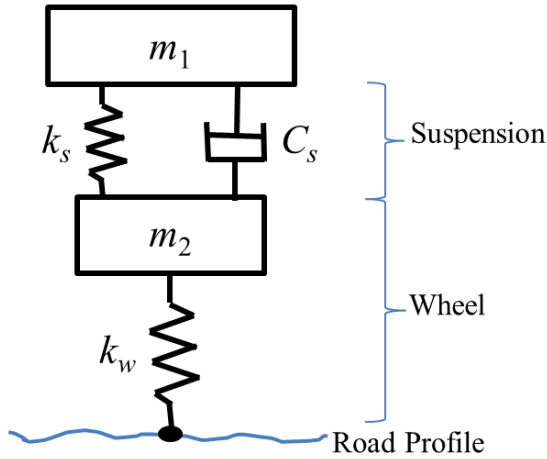


Figure 3. Q-car model

The equations of motion for the vehicle are described in detail by Cantero et al (2009), and similarly to the equations of the bridge, they can be expressed in matrix form as:

$$[M_v]\{\ddot{w}_v\} + [C_v]\{\dot{w}_v\} + [K_v]\{w_v\} = \{f_v\} \quad (6)$$

where $[M_v]$, $[C_v]$ and $[K_v]$ are global mass, damping and stiffness matrices of the vehicle respectively, $\{w_v\}$, $\{\dot{w}_v\}$ and $\{\ddot{w}_v\}$ are the vectors of global displacements, their velocities and accelerations respectively, and $\{f_v\}$ is the vector of forces acting on the vehicle at time t . The model assumes vertical tyre-ground contact forces at single points, constant vehicle speed, driving path in a straight line, and negligible lateral and yaw motions.

2.3 Vehicle-bridge interaction algorithm

There are two sets of differential equations of motion, one set defining the DOFs of the bridge and the other the DOFs of the vehicle. To analyse the VBI problem it is necessary to solve both subsystems while ensuring compatibility at contact points. The algorithm used to carry out this calculation is based on an uncoupled iterative procedure where equations of motion of the bridge and vehicle are solved separately and equilibrium between both sub-

systems and geometric compatibility conditions are found through an iterative process. The basic idea behind this procedure consists of assuming some initial displacements for the contact points, which can be replaced in the equations of motion of the vehicle to obtain the interaction forces. Then these interaction forces are employed in the equations of motions of the bridge to obtain the bridge displacements ($w_b(x,t+1)$) that will represent improved estimates of the initial displacements ($w_b(x,t)$) assumed for the contact points. The process is repeated until differences in two successive iterations are sufficiently small. This algorithm employs the Newmark-Beta direct integration method to solve each subsystem and to achieve convergence after a number of iterations. This is an implicit direct integration scheme, where the dynamic response of the structure is solved at a particular point in time, using values of the dynamic variables at both the current and previous time steps (Tedesco 1999). Full details of the algorithm iterative process can be found in González (2011).

The program model is set so that convergence occurs if

$$\frac{\max(w_b(x,t+1) - w_b(x,t))}{\max(w_b(x,t+1))} \times 100 < 0.1 \quad (7)$$

Once convergence has been achieved, the simulation of the acceleration signal, at any point on the bridge, can be extracted and subjected to further signal processing.

3 SIGNAL PROCESSING

The signal processing technique used is a 2-step procedure, firstly a Moving Average Filter (MAF) is applied to the signal and secondly, EMD is carried out on the filtered signal.

3.1 Moving Average Filter

The simulated damage will reveal as a local discontinuity in the acceleration signal as the load crosses the bridge. This acceleration signal is made up of three component parts; the 'static', 'damage' and 'dynamic' components. The 'static' component increases linearly from zero to a maximum at the monitored location and then decreases linearly back to zero while, the 'damage' component is zero everywhere except at the damage location. Therefore by applying an appropriate filtering method to the acceleration signal, it is possible to remove its dynamic component and locate damage in a bridge (Hester & González, 2010). The MAF has been found to be a suitable filtering method for this purpose.

A MAF replaces each point in the signal with an average of several adjacent points. The acceleration signal vibrates primarily at one frequency, associated to the main mode of vibration of the bridge, and therefore the dynamic oscillations can be removed by setting the span of the filter equal to one period of vibration. In practice, a fast Fourier transform of the acceleration signal can be used to obtain the dominant frequency, that will be subsequently used to calculate the span required for the MAF. The filter removes the dominant frequency of the bridge, while smoothing higher frequencies associated to modes of vibration of the structure, the static component and any discontinuities. When applying the MAF, the number of data points obtained will be reduced by the span of the filter and the location of the discontinuities will be altered. To allow for this the signal is relocated to start one half span distance from the first support. Figure 4 is an example of a damaged acceleration signal after undergoing the filtering process. For this example, a 10 tonne vehicle is crossing at 5 m/s and the damage is modelled as a 30% reduction in stiffness, across the width of the bridge, at 12 m. This figure clearly shows the triangular shape of the ‘static’ component along with the ‘damage’ component which occurs as a spike at 2.4 s, the time that the vehicle reaches the damage point.

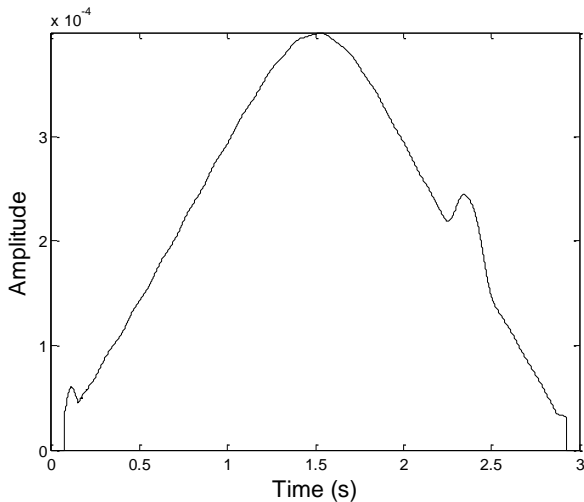


Figure 4. Acceleration signal after applying MAF

3.2 Empirical Mode Decomposition

EMD is a signal processing method which decomposes data into several IMFs by a procedure known as the sifting process. Huang & Shen (2005) provide a detailed description of the EMD process. The first IMF contains the highest frequency components in the signal and therefore, by the removal of the low frequency elements, highlights any high frequency discontinuities that may occur in a signal.

Once the MAF has been applied to the signal, EMD is next employed to obtain the first IMF. This creates a monocomponent signal which has a zero mean. Applying EMD reduces the presence of the static component of the signal which, remains after filtering as a triangular shape and leaves mainly the damage component of the signal, Figure 5. The peaks obtained above the zero mean line in the first IMF considerably magnify the presence of damage compared to just employing the MAF, see Figure 4, particularly with the occurrence of low levels of damage.

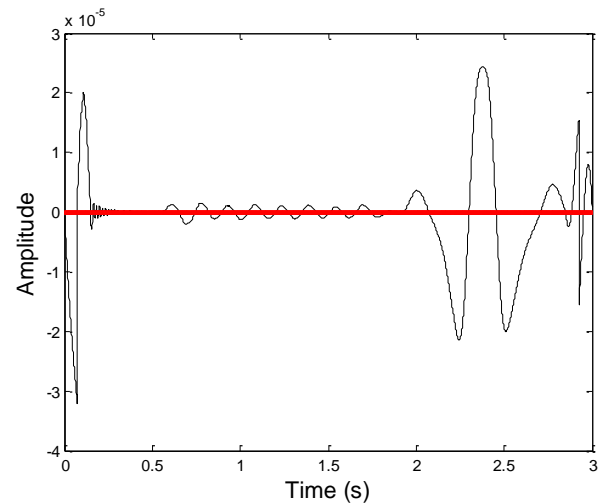


Figure 5. IMF 1 of Figure 4

4 TESTING RESULTS

The effects that the level of damage, road surface smoothness, vehicle speed, vehicle load and sensor location have on the accuracy of the proposed signal processing technique are examined here. Unless specified otherwise, the acceleration signal is taken from the midpoint on the bridge (i.e., longitudinal position of 7.5 m at the bridge centerline).

4.1 Influence of size and location of damage

The ability of the signal processing procedure to detect a reduction in stiffness of 50, 30 and 10% was examined using a perfectly smooth road profile and a vehicle weighing 10 tonne, moving at a speed of 5 m/s. Damage was first assumed to cover the full width of the bridge at a longitudinal position of 12 m (3/5 of the total span) from the start of the bridge. Figure 6 shows IMF 1 after applying the MAF followed by EMD. The horizontal axis shows time from the instant the vehicle enters the bridge, which means the damage should be located at 2.4 s.

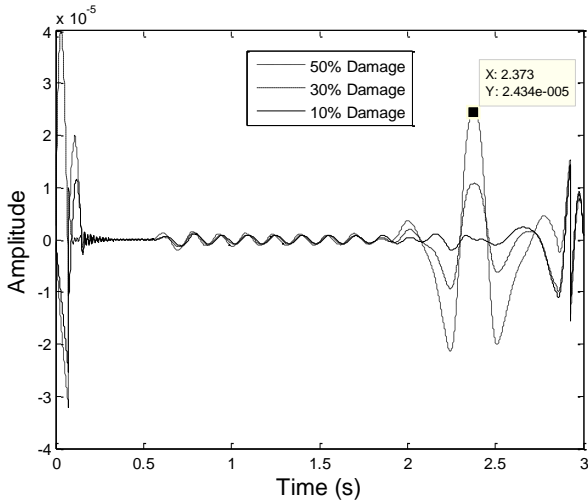


Figure 6. IMF 1 results

Peaks in these results are clear for 50 and 30% damage, however, 10% damage cannot be easily detected. Using the acceleration signal obtained at a location 10 m along the bridge centerline (i.e 2.5 m closer to the damage location than in Figure 6), allows damage of 10% to be detected as shown in Figure 7, however the results are still not as clear as for higher levels of damage.

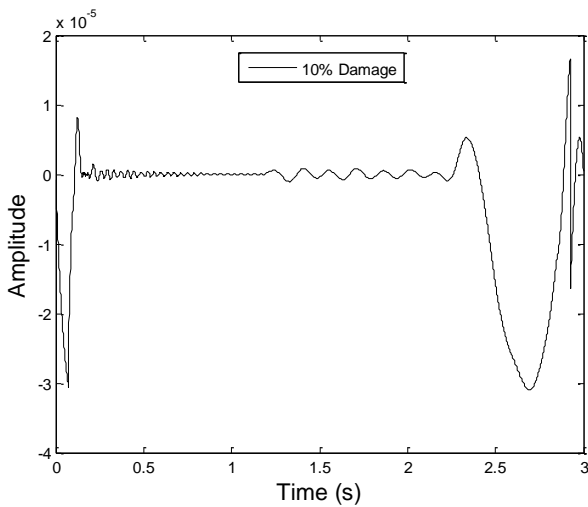


Figure 7. IMF 1 of filtered acceleration signal obtained at 10 m on a bridge with 10% loss stiffness at 12 m

Next, as it is unlikely to find damage through the full width of a bridge, two small isolated damaged portions were separately examined. Both damaged locations were at a longitudinal position of 12 m from the start of the bridge, but located at different transverse locations of 1 m and 6 m in from the edge. Both damage locations contain two adjacent damaged elements in the transverse direction, i.e they are 0.25 m long and 0.5 m wide. All vehicle and road properties remained the same as the previous model. It was initially found that these small sections of damage could not be detected, however on further testing it was discovered that for damage to be detected it was necessary for the wheel run to cross over the damage location.

The results shown in Figure 8 are for damage located from 1 m to 1.5 m from the edge, the reduction in stiffness is 50% and different locations of the wheel run are illustrated. Damage can only be detected where the run of the wheel crossed the damage location, i.e, at 1.5 m. The same results occurred for the damage located at 6 m from the edge of the bridge.

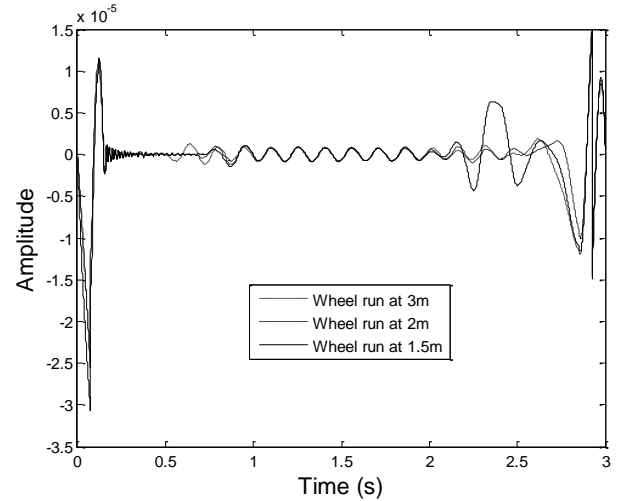


Figure 8. Results for varying wheel run locations

4.2 Influence of road surface smoothness

As all test results up to this point have been for a perfectly smooth road profile, it is now important to examine results with profiles set to ISO standards. A class 'A' profile ($G_d(n_0) \leq 2 \times 10^{-6} \text{ m}^3/\text{cycle}$) was first modelled with vehicle properties remaining the same as previous models. The damage is again located across the full width of the bridge at 12 m and the acceleration signal is obtained from the centre of the bridge. Figure 9 shows that it is not possible to determine the damage location at 2.4 s with a load of 10 tonnes moving at 5 m/s. Larger loads were then tested, and Figure 10 shows how a load of 50 tonne appears to be sufficient to identify 30% damage in this particular case.

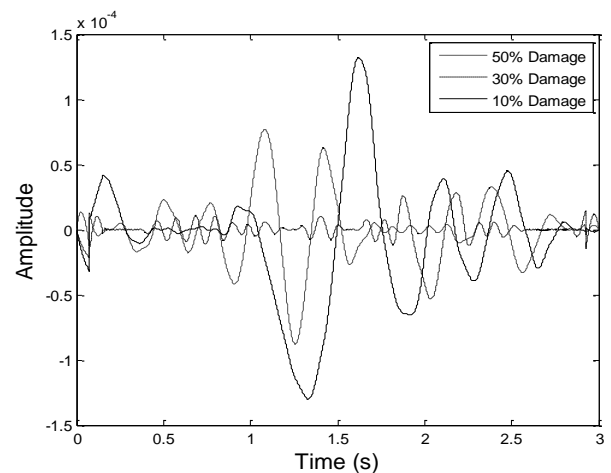


Figure 9. Class 'A' profile with 10 tonne load

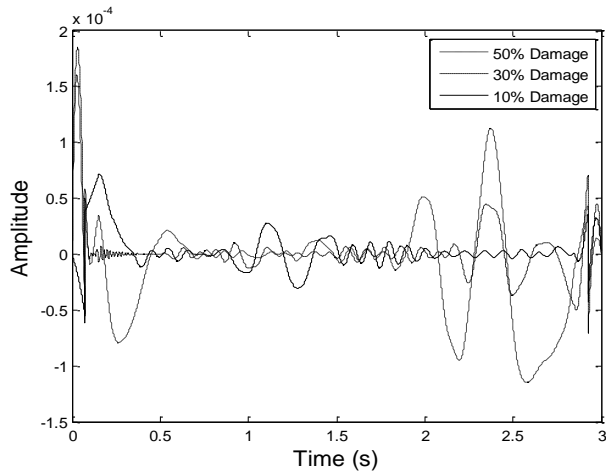


Figure 10. Class 'A' profile with 50 tonne load

Finally a class 'B' profile is tested ($2 \times 10^{-6} < G_d(n_0) \leq 8 \times 10^{-6} \text{ m}^3/\text{cycle}$). Here, loads that could be sufficient to detect damage in class 'A' profiles, are unable to locate damage due to the increasing difficulty in capturing damage as the road gets rougher. Figure 11 shows how a load of 200 tonne appears to be sufficient to detect 30% damage in a class 'B' road.

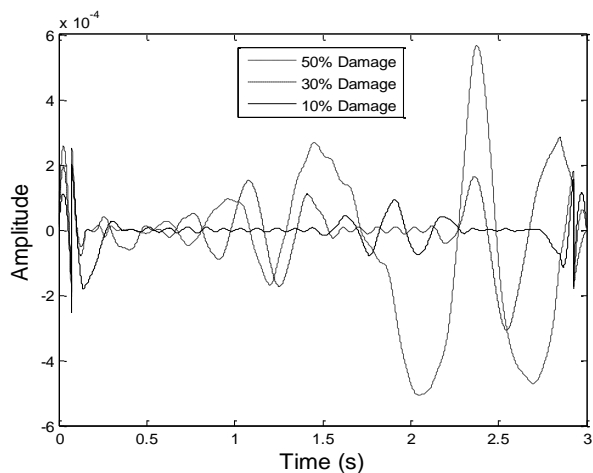


Figure 11. Class 'B' profile with 200 tonne load

4.3 Influence of vehicle speed

It is found that the lower the speed the sharper the damage peak is, however the peaks become broader with increased speed due to the reduction in the wave frequency and increase in wavelength. At speeds of 15 m/s and above the occurrence of damage is still clear however the accuracy in locating the damage is reduced. The increase in wavelength of the acceleration signal makes detection of the frequency shift location less accurate. The results in Figure 12 are for a vehicle travelling at 10 m/s on a smooth road profile. Three bridge models are shown with losses in stiffness of 50, 30 and 10% at 12 m.

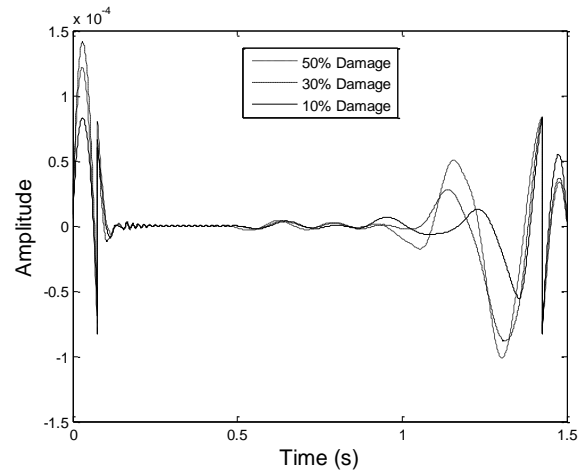


Figure 12. IMF 1 for vehicle travelling at 10 m/s

4.4 Influence of sensor location

Finally, the influence on the sensor location on the ability to detect damage is examined. Up to this point, the sensor has been located at the midpoint of the bridge. Testing has shown that locating the sensor transversely close to the path of the vehicle causes a peak to occur at the point where the vehicle passes the sensor location as well as at the damage location (i.e., at 1.5 and 2.4 s in Fig. 13).

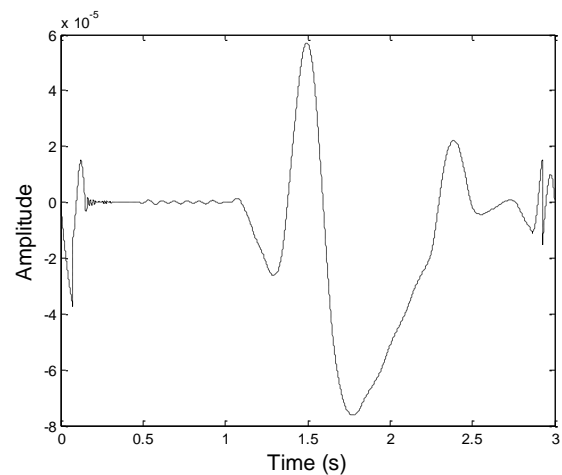


Figure 13. Sensor located along vehicle path

This non-damage peak can make the existence of damage close to the sensor location difficult to distinguish and therefore it was determined that the sensor should be located in excess of 2 m to either side of the wheel path to remove this extra peak. The effect of the longitudinal distance of the sensor from the damage is shown in Figure 14. For this example a 10 tonne vehicle is crossing at 5 m/s and the damage is modelled as a 30% reduction in stiffness, across the width of the bridge, at 12 m. In this figure, it can be seen that, sensors situated closer to the damage location will produce higher peaks than those further away. For this bridge model, it is found that beyond a distance of 6 m it becomes difficult to detect damage occurrences.

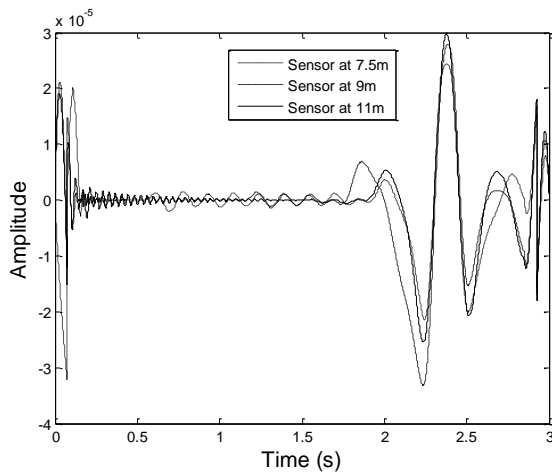


Figure 14. Effect of longitudinal distance between sensor and damage

5 CONCLUSION

It is desirable that bridge damage detection techniques employ operating loads, such as vehicular loads, as excitation sources, which do not require controlled vibration conditions, a perfect knowledge of the excitation source or closure of the structure. This paper has proposed a health monitoring technique with the potential to be used with everyday operating loads, and to identify and locate damage with minimal use of resources.

Testing of the technique has been carried out here using simulations from a quarter-car vehicle-bridge dynamic interaction finite element model. It was found that the method is capable of detecting a loss in stiffness as low as 10 %, however to detect this level the vehicle must cross the damage location. It was also found that an increase in road roughness made detection more difficult, requiring larger vehicle loads and an increase in vehicle speed has an effect on the accuracy of locating the damage. This approach, however, is shown to be a promising tool for damage detection of real structures with relatively low-costs and simple implementation.

ACKNOWLEDGEMENTS

This research is supported by a scholarship from the Irish Research Council for Science, Engineering and Technology (IRCSET).

REFERENCES

Ayenu-Prah, A., Attoh-Okine, N. 2009. Comparative study of Hilbert-Huang transform, Fourier transform and Wavelet transform in pavement profile analysis. *Vehicle System Dynamics* 47: 437-456.

- Bradley, M., González, A. & Hester, D. 2010. Analysis of the structural response of a moving load using Empirical Mode Decomposition. In *Proceedings of the 5th International Conference on Bridge Maintenance, Safety, Management and Life-Cycle Optimization, IABMAS2010*: 356-363. Philadelphia.
- Cantero, D., O'Brien, E. J. & González, A. 2009. Modelling the vehicle in vehicle-infrastructure dynamic interaction studies. *Proceedings of the Institution of Mechanical Engineers, Part K: Journal of Multi-body Dynamics*. 243-248.
- González, A. 2011. Chapter 'Vehicle-Bridge Dynamic Interaction Using Finite Element Modelling' in *Finite Element Analysis*, ISBN: 978-953-307-123-7, Editor David Moratal, Croatia, Sciyo. 637-662.
- González, A., Hester, D. 2009. The use of wavelets on the response of a beam to a calibrated vehicle for damage detection. *The e-Journal & Exhibition of Nondestructive Testing*. ID:7761.
- Hester, D. & González, A. 2010. Detecting damage in a beam subject to a moving load using localised variation in vibration response. In *Proceedings of Bridge and Infrastructure Research in Ireland, BCRI2010*: 307-314. Cork.
- Harris, N. K., O'Brien, E. J., González, A. 2007. Reduction of bridge dynamic amplification through adjustment of vehicle suspension damping. *Journal of Sound and Vibration* 302:471-485.
- Huang, K. 2001. *Structure Safety Inspection*. United States Patent, US 6192758 B1.
- Huang, N.E. & Shen, S.S. 2005. *Hilbert-Huang transform and its applications*. London, World Scientific.
- ISO 8608. 1995. Mechanical vibration – road surface profiles – reporting of measured data, BS 7853:1996, ISBN 0-580-25617-0, London.
- Kim, H. & Melhem, H. 2004. Damage detection of structures by Wavelet analysis. *Engineering Structures* 26(3):347-362.
- Meredith, J. & González, A. 2011. Damage identification in bridges using Empirical Mode Decomposition of the acceleration response to random traffic. In *Proceedings of Innovations on Bridges and Soil-Bridge Interaction, IBSBI2011*. Athens, Greece.
- Meredith, J., González, A. & Hester, D. 2011. Empirical Mode Decomposition of the acceleration response of a prismatic beam subject to a moving load to identify multiple damage locations. In *Proceedings of the International Conference on Structural Engineering Dynamics, ICEDyn2011*. Tavira, Portugal.
- O'Brien, E.J., Cantero, D., Enright, B. & González, A. 2010. Characteristic dynamic increment for extreme traffic loading events on short and medium span highway bridges. *Engineering Structures* 32(12):3827-3835.
- Salvino, L.W., Pines, D.J., Todd, M. & Nichols, J.M. 2005. EMD and instantaneous phase detection of structural damage. *Hilbert-Huang Transform and Its Applications*, Chapter 11 227-259
- Tedesco, J. W., McDougal, W. G., & Allen Ross, C. 1998. *Structural Dynamics: Theory and applications*. California, Addison Wesley Longman. Inc.
- Yang, J.N., Lei, Y., Lin, S. & Huang, N. 2004. Hilbert-Huang based approach for structural damage detection. *Journal of Engineering Mechanics*. 130(1):85-95.
- Xu, Y.L., Chen, J. 2004. Structural damage detection using Empirical Mode Decomposition: Experimental Investigation. *Journal of Engineering Mechanics* 130(11):1279-1288.
- Zhu, X., Law, S. 2006 Wavelet-based crack identification of bridge beam from operational deflection time history. *International Journal of Solids and Structures* 43(7-8): 2299-2317.